Journal of Power Sources 223 (2013) 254–258

Contents lists available at SciVerse ScienceDirect

Journal of Power Sources

journal homepage: www.elsevier.com/locate/jpowsour

Short communication

Enhanced conversion efficiency of dye-sensitized solar cells using Sm_2O_3–modified TiO_2 nanotubes

Rui Liu [a], Liang-Sheng Qiang [a,*], Wein-Duo Yang [b,**], Hsin-Yi Liu [b]

[a] Department of Applied Chemistry, Harbin Institute of Technology, Harbin 150001, PR China
[b] Department of Chemical and Materials Engineering, National Kaohsiung University of Applied Sciences, Kaohsiung 807, Taiwan

HIGHLIGHTS

- We fabricate Sm_2O_3/TiO_2 nanotubes as photo-anode in DSSCs.
- Sm_2O_3 as luminescence conversion material can improve the UV radiation harvesting to increase current.
- The results show that efficiency of DSSCs improves by 73.1% under optimum condition.

ARTICLE INFO

Article history:
Received 10 May 2012
Received in revised form
8 August 2012
Accepted 14 September 2012
Available online 20 September 2012

Keywords:
Titania nanotubes
Dye-sensitized solar cells
Samarium oxide
Luminescence

ABSTRACT

Highly ordered TiO_2 nanotubes grown on a Ti substrate are conveniently modified with samarium oxide (Sm_2O_3) by a hydrothermal method for use in back-illuminated dye-sensitized solar cells. As a down-conversion luminescence material, samarium oxide improves the UV radiation harvesting and thus increases the photocurrent. The results show that Sm_2O_3–modified TiO_2 nanotubes can increase the short-circuit current and the conversion efficiency of dye-sensitized solar cells. When TiO_2 nanotubes are modified by 0.02 M Sm_2O_3, the efficiency is improved by 73.1% compared with bare TiO_2 nanotubes.

1. Introduction

Since Grätzel and O'Reagan proposed TiO_2-based dye-sensitized solar cells (DSSCs), which are low-cost and have high photo-conversion efficiencies [1], DSSCs have attracted significant attention. Recently, more and more researchers have devoted their attention to one-dimensional TiO_2 nanotube-based DSSCs because of their capabilities in terms of electron lifetime and electron transport [2,3]. However, the conversion efficiency of DSSCs is not ideal due to low light harvesting. DSSCs contain dye molecules, an electrolyte, a TiO_2 anode and a Pt counterelectrode. Most dyes (N719, N3, etc) only absorb visible light ranging from approximately 290–800 nm, so most of the solar ultraviolet irradiation is not used [4]. If solar ultraviolet irradiation can be transformed to visible light by a down-conversion luminescence material [5–8], more sun irradiation will be absorbed by sensitized dyes, improving the light harvesting thus enhancing the conversion efficiency of DSSCs. Lanthanide-derived compounds have been widely used as efficient light conversion molecular devices due to their specific 4f electronic structure and unique properties [9–11]. Among the lanthanide ions, samarium (Sm^{3+}) ions have been considered to be the most efficient down-converting material, which can absorb ultraviolet light to visible light [12–15]. However, there are few reports about lanthanide ion modification of one-dimensional TiO_2 nanotubes for application to DSSCs.

In this work, highly ordered TiO_2 nanotubes grown on a Ti substrate are modified by Sm_2O_3 with a hydrothermal method for use as the photo-anode of dye-sensitized solar cells. We have investigated the properties and performance of different concentrations of Sm_2O_3/TiO_2 nanotubes to improve the photocurrent and the conversion efficiency.

2. Experimental

2.1. Preparation of Sm_2O_3–modified TiO_2 nanotubes

Highly ordered TiO_2 nanotubes were prepared using anodization of titanium foils at 50 V for 8 h under magnetic stirring, as

* Corresponding author.
** Corresponding author. Tel.: +886 73814526x5116; fax: +886 73830674.
E-mail addresses: qiangls@sina.com (L.-S. Qiang), ywd@cc.kuas.edu.tw (W.-D. Yang).

0378-7753/$ – see front matter © 2012 Elsevier B.V. All rights reserved.
http://dx.doi.org/10.1016/j.jpowsour.2012.09.045

previously reported [16]. The electrolyte contained ethylene glycol, 0.3 wt% ammonium fluoride and 2 vol% water. Sm_2O_3–modified TiO_2 electrodes were fabricated using a hydrothermal method. The TiO_2 nanotubes were dipped into 0.01 M, 0.02 M, 0.03 M and 0.05 M $Sm(NO_3)_3$ solution, respectively, then heated to 100 °C for 12 h in a Teflon container. Lastly, they were annealed at 550 °C in a furnace for 1 h (10 °C min^{-1} heating temperature). The modified samples were marked as Sm_2O_3/TiO_2 nanotubes.

2.2. Fabrication DSSCs

The prepared TiO_2 nanotubes and different concentrations of Sm_2O_3/TiO_2 nanotubes were immersed in a 0.5 mM solution of N719 dye at 70 °C for 24 h. The nanotubes were washed in ethanol to remove nonchemisorbed dye and dried in an oven. A hot-melt polymer (Solaronix SX1170-25, 60 μm) was used as an adhesive spacer. The liquid electrolyte is composed of 0.1 M LiI, 0.05 M I_2 and 0.5 M 4-*tert*-butylpyridine (TBP) in acetonitrile. The electrolyte was injected between two electrodes and was driven through holes in the hot-melt sealing foil by capillary force. The platinum counter-electrode was prepared by spin-coating: the FTO was fixed in a spin coating (WS-400A-6NPP/LITE), a mixture of 5 mM H_2PtCl_6 and ethanol was dropped onto FTO at 1000 rpm for 40 s and then calcined at 385 °C for 10 min. The TiO_2 electrode and the counterelectrode were appropriately spaced and sealed using a hot-melt film as a sandwich spacer.

2.3. Characterization

The crystal structures of the samples were characterized by X-ray diffraction (XRD, PANalytical/X'Pert PRO MPD) using Cu Kα ($\lambda = 0.154$ nm) radiation at 10 kV and 100 mA; the samples were scanned from 20 to 80°. The morphologies were observed with a field-emission scanning electron microscope (FESEM, JEOL JSM-7401F) at 5 kV and an amplification ratio of 50,000 and connected to an EDX detector. The photoluminescence spectra were obtained using a fluorescence spectrometer (F-4500). The UV–vis diffuse reflection spectrum of the sample was measured with a UV–Vis 2550 spectrophotometer. The photocurrent–voltage characteristics were measured under simulated solar light (AM 1.5, 100 mW cm^{-2}) using a Keithley 2400 sourcemeter; the active area of the solar cells was 0.25 cm^2.

3. Results and discussions

3.1. Structure and morphology properties

Fig. 1(a) shows the pure TiO_2 nanotubes with an ordered surface morphology and a 98 nm inner diameter. The inset of Fig. 1(a) shows a vertical tube with a length of approximately 13 μm. Similar images were obtained for different concentrations of Sm_2O_3/TiO_2 nanotubes; the 0.02 M Sm_2O_3/TiO_2 nanotubes are shown in Fig. 1(b). The surface morphology changed little. EDX were employed to investigate the elemental composition of TiO_2 and the modified TiO_2 nanotubes. Fig. 1(c) shows strong diffraction peaks at 4.5 keV and 4.9 keV from Ti, while 0.5 keV is ascribed to O. Ti, O and Sm were detected for 0.02 M Sm_2O_3/TiO_2 nanotubes, as shown in Fig. 1(d), which confirms the presence of Sm_2O_3 on the surface of TiO_2 nanotubes.

Fig. 2 shows the XRD patterns of TiO_2 nanotubes and different concentrations of Sm_2O_3/TiO_2 nanotubes. The characteristic peaks at 25.40° and 48.04° can be assigned to the (101) and (200) planes of the anatase phase, respectively. After modification, no Sm_2O_3 peak is observed, which is similar to bare TiO_2 nanotubes. This indicates that the modification has no influence on the crystalline phase of the TiO_2 nanotubes. The absence of the Sm_2O_3 peak may be due to the low Sm_2O_3 amount or the high dispersity. A broader peak and a blue shift for the (101) plane occur with increasing concentrations of Sm_2O_3. The values of the peak broadness and the peak height of the (101) plane are shown in Table 1. The peak of the

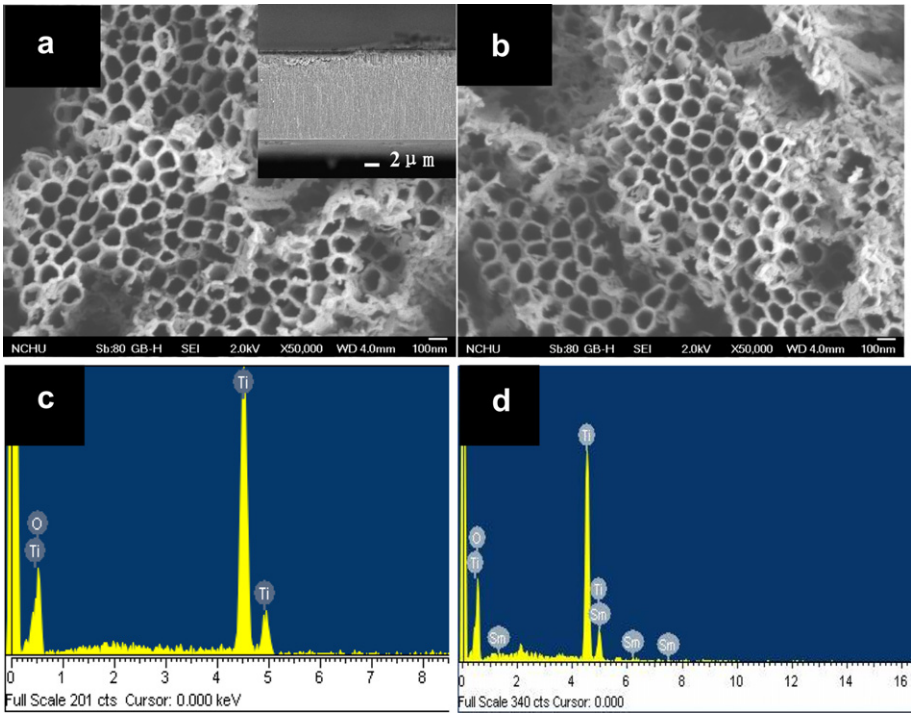

Fig. 1. (a) FESEM images of TiO_2 nanotube arrays, (b) top view of FESEM images of 0.02 M Sm_2O_3/TiO_2 nanotubes, (c) EDX spectrum of TiO_2 nanotube arrays, (d) EDX spectrum of 0.02 M Sm_2O_3/TiO_2 nanotubes.

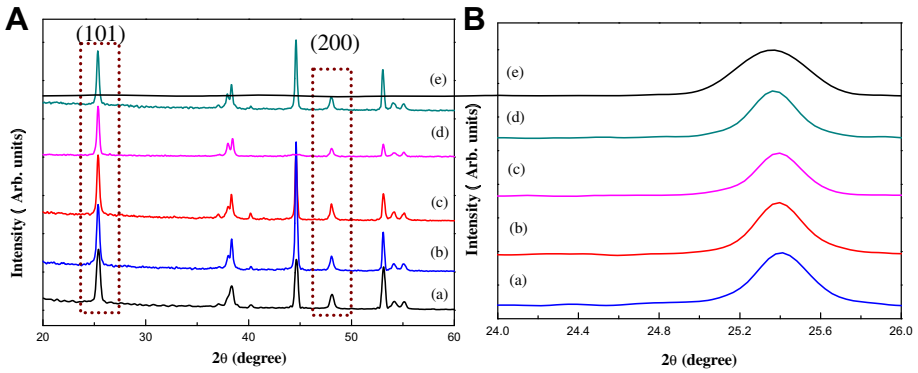

Fig. 2. (A) XRD patterns of TiO_2 nanotubes and different concentrations of Sm_2O_3/TiO_2 nanotubes. (B) Enlarged XRD patterns of (101) planes: (a) TiO_2 nanotubes, (b) 0.01 M Sm_2O_3/TiO_2 nanotubes, (c) 0.02 M Sm_2O_3/TiO_2 nanotubes, (d) 0.03 M Sm_2O_3/TiO_2 nanotubes, (e) 0.05 M Sm_2O_3/TiO_2 nanotubes.

(101) plane is also demonstrated in Fig. 1(B) more clearly. The increase in the full width at half maximum is due to the smaller grain size [17]. The slight blue shifts of the 25.40° peak are observed with increasing concentrations of Sm_2O_3, which confirms that a small amount of Sm has entered the lattice of the TiO_2 nanotubes. However, because the Sm^{3+} (0.96 Å) radius is much larger than the Ti^{4+} radius (0.68 Å), Sm^{3+} cannot replace the Ti^{4+} in the lattice but rather exists in the lattice interstitial voids. It is assumed that a small amount of Sm^{3+} exists in the lattice of the TiO_2 nanotubes due to the slight blue shift.

3.2. Optical properties

Fig. 3 shows the UV–vis diffuse reflection spectrum of TiO_2 and different concentrations of Sm_2O_3/TiO_2 nanotubes. The absorption edge for TiO_2 nanotubes is approximately 372.0 nm, which is ascribed to charge transfer from the 2p orbit of O to the 3d orbit of Ti. After modification, the absorption edge moved to a higher wave number with the increasing concentration of Sm_2O_3, especially in 0.03 M and 0.05 M Sm_2O_3/TiO_2 nanotubes, which is related to the charge transfer from the 2p orbit of O^{2-} to the 4f orbit of Sm^{3+}. As seen from the ultraviolet absorption band, it is confirmed that Sm_2O_3/TiO_2 nanotubes can absorb ultraviolet light from the sun [18]. Moreover, the higher the absorption edge is, the narrower the bandgap will be, which is beneficial for inducing excited dye electron injection into the conduction band of TiO_2 in dye-sensitized solar cells.

Fig. 4 shows the excitation spectrum (A) and the emission spectrum (B) of 0.02 M Sm_2O_3/TiO_2 nanotubes. Fig. 4(A) exhibits a peak at approximately 371.9 nm in the ultraviolet region, in accordance with the absorption spectrum (approximately 372.1 nm), which indicates energy transfer from TiO_2 to Sm^{3+}. The weak band at 421.2 nm is ascribed to the direct excitation of Sm^{3+}. The bands of emission shown (B) at 587 nm, 613 nm and 664 nm are the electronic transition of $^4G_{5/2}$-$^6H_{5/2}$, $^4G_{5/2}$-$^6H_{7/2}$ and $^4G_{5/2}$-$^6H_{9/2}$ of Sm^{3+} [19,20], which is within the absorption wavelength range of N719 dye. Therefore, ultraviolet light from the sun can be reabsorbed by N719 dye via down-conversion luminescence from Sm^{3+}, which can improve the light-harvesting ability of DSSCs.

Table 1
The values of full width half maximum and peak height of (101) peaks.

Samples	Peak position (°)	FWHM (°)	Peak height (counts)
TiO_2 nanotubes	25.40	0.36	153.5
0.01 M Sm_2O_3/TiO_2 nanotubes	25.38	0.36	153.5
0.02 M Sm_2O_3/TiO_2 nanotubes	25.37	0.36	152.8
0.03 M Sm_2O_3/TiO_2 nanotubes	25.36	0.38	151.2
0.05 M Sm_2O_3/TiO_2 nanotubes	25.34	0.40	151.0

3.3. Conversion efficiency of DSSCs

Fig. 5 depicts the *I–V* characteristics of DSSCs for TiO_2 nanotubes and different concentrations of Sm_2O_3/TiO_2 nanotubes, and the corresponding values are summarized in Table 2. For the bare TiO_2 nanotubes, the DSSCs exhibited a J_{sc} value of 5.64 mA cm^{-2}, a V_{oc} value of 0.580 V and a fill factor (FF) of 0.570, yielding an overall conversion efficiency of 1.86%. When 0.01 M Sm_2O_3–modified TiO_2 nanotubes are used, J_{sc} and the performance of the DSSCs are improved. Here, the dye absorption has been increased for Sm_2O_3/TiO_2 nanotubes because a Ti–O–Sm complex is formed between the Sm_2O_3 and TiO_2 nanotubes, which generates an imbalance in the lattice charge. To make up for the imbalance, some –OH are absorbed on the surface of TiO_2 nanotubes to improve the hydrophilicity. As a result, the dye absorption is slightly increased. However, J_{sc} obviously increased, primarily because the conversion luminescence of Sm^{3+} can change ultraviolet light into visible light so that more incident light can be harvested, as confirmed by the PL measurements. When the concentration of Sm^{3+} is 0.02 M, the J_{sc}

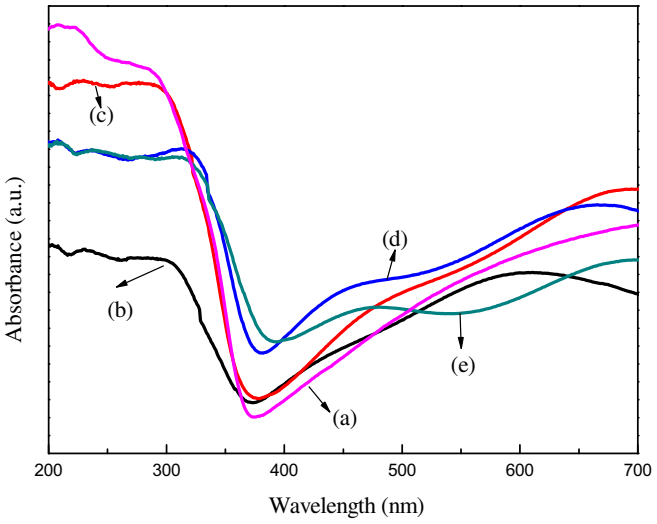

Fig. 3. UV–vis RDS spectra of TiO_2 nanotubes and different concentrations of Sm_2O_3/TiO_2 nanotubes: (a) TiO_2 nanotubes, (b) 0.01 M Sm_2O_3/TiO_2 nanotubes, (c) 0.02 M Sm_2O_3/TiO_2 nanotubes, (d) 0.03 M Sm_2O_3/TiO_2 nanotubes, (e) 0.05 M Sm_2O_3/TiO_2 nanotubes.

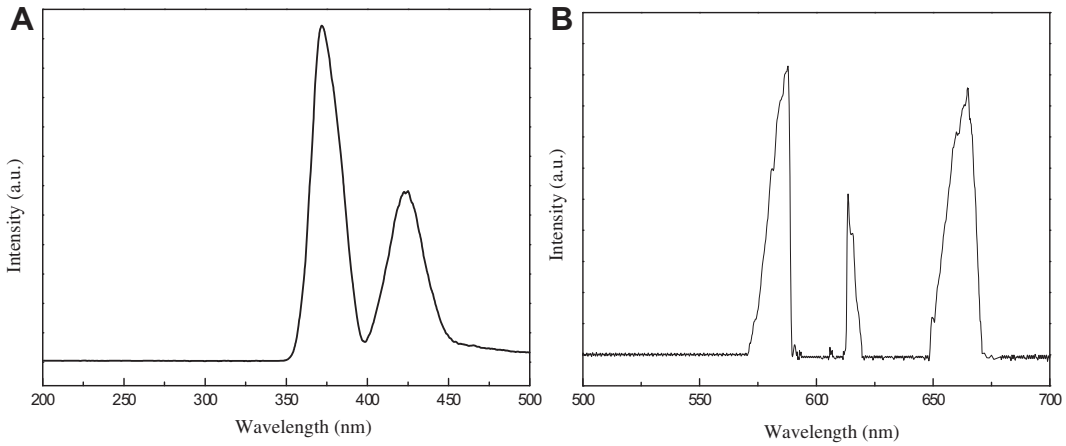

Fig. 4. (A) Excitation spectra of 0.02 M Sm_2O_3/TiO_2 nanotubes (λ_{em} = 613 nm) and (B) emission spectra of 0.02 M Sm_2O_3/TiO_2 nanotubes (λ_{ex} = 370 nm).

reached its maximum value, which gives an efficiency of 3.22%, namely, an increase of 73.1% compared with unmodified TiO_2 nanotubes. The V_{oc} is slightly improved with increasing concentrations of Sm^{3+}. This result may be explained by the fact that most Sm^{3+} ions cannot enter the lattice and thus coat the surface of TiO_2 nanotubes with a type of Sm_2O_3, which is treated as an energy barrier that decreases the chance of charge recombination. However, the short-circuit current and conversion efficiency decreases as the concentration of Sm^{3+} increases. The decrease primarily occurs because the structure of TiO_2 nanotubes is distorted by too many Sm^{3+} ions in the lattice interstitial voids, consequently producing some crystal defects, which capture photo-induced electrons, leading to a decrease in current. When the concentration of Sm^{3+} increased to 0.05 M, J_{sc} decreased obviously, while V_{oc} increased. This may occur because the distortion and expansion of the lattice caused the O atom to escape from the lattice containing too much Sm^{3+}, leading to oxygen vacancies. The defect equation can be written as follows:

$$2Ti_{Ti} + 4O_o \rightarrow 2Ti_{Ti}^{\cdot\cdot} + V_o^{\cdot\cdot} + 3O_o + 1/2O_2$$

The oxygen vacancies can reduce the recombination of the electron-hole to extend the electron lifetime, thus improving V_{oc}.

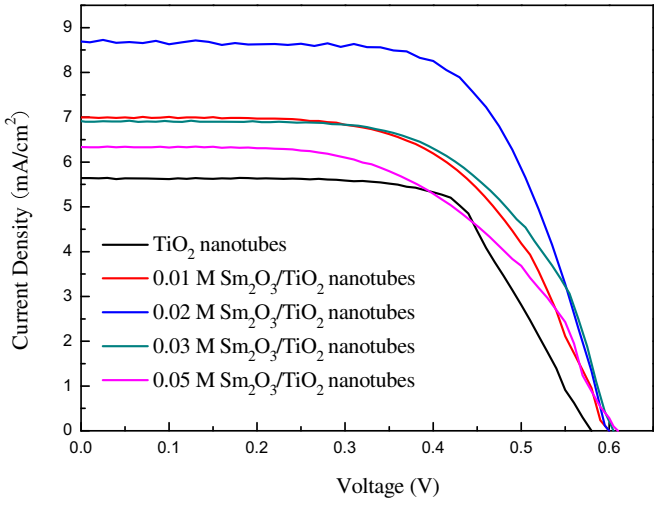

Fig. 5. Photocurrent–voltage (I–V) characteristics of dye-sensitized TiO_2 nanotubes and different concentrations of Sm_2O_3/TiO_2 nanotubes.

Table 2
Photovoltaic performance of DSSCs under AM-1.5 illumination.

Photoanode	V_{oc} (V)	J_{sc} (mA cm^{-2})	FF	η (%)	Dye loading (mol cm^{-2})
TiO_2 nanotubes	0.580	5.64	0.570	1.86	6.58×10^{-8}
0.01 M Sm_2O_3/TiO_2 nanotubes	0.600	7.00	0.617	2. 59	7.36×10^{-8}
0.02 M Sm_2O_3/TiO_2 nanotubes	0.600	8.67	0.619	3.22	7.73×10^{-8}
0.03 M Sm_2O_3/TiO_2 nanotubes	0.605	6.90	0.615	2.57	7.70×10^{-8}
0.05 M Sm_2O_3/TiO_2 nanotubes	0.610	6.33	0.585	2.26	7.29×10^{-8}

The fill factor, which is related to internal resistance, is also an important factor for improving the efficiency of DSSCs. If the series resistance is decreased, the fill factor is increased. A proper energy barrier layer can disperse Sm_2O_3 at the interface to increase electron transport. Therefore, if the resistance is reduced, to a certain extent, the fill factor will increase.

4. Conclusion

In conclusion, we have prepared highly ordered TiO_2 nanotubes modified with samarium oxide that were used as photo-anodes in DSSCs and that exhibited excellent performance. This result indicates that Sm_2O_3 is not only serving as a down-conversion luminescence material to increase the photocurrent but also that it can be considered an energy barrier on the surface of TiO_2 nanotubes to increase the photovoltage. With 0.02 M Sm_2O_3–modified TiO_2 nanotubes, the conversion efficiency increased by 73.1% compared with bare TiO_2 nanotubes. This finding verifies that using Sm_2O_3 as a luminescence medium in dye-sensitized solar cells is an efficient method to increase the conversion efficiency. Further optimizations, such as the use of a longer tube and a front illumination method, are expected to further increase the conversion efficiency.

References

[1] B. O'Regan, M. Grätzel, Nature 353 (1991) 737–739.
[2] G.K. Mor, K. Shankar, M. Paulose, O.K. Varghese, C.A. Grimes, Nano Lett. 6 (2006) 215–218.
[3] M. paulose, G.K. Mor, O.K. Varghese, K. Shankar, C.A. Grimes, J. Photochem. Photobiol. A 178 (2006) 8–15.
[4] M. Grätzel, Nature 414 (2001) 338–344.
[5] H. Hafez, J.H. Wu, Z. Lan, Q.H. Li, G.X. Xie, Nanotechnology 21 (2010) 415201 1–6.
[6] M. Grätzel, Inorg. Chem. 44 (2005) 6841–6851.
[7] S. Bingham, W.A. Daoud, J. Mater. Chem. 21 (2011) 2041–2050.
[8] M. Pal, U. Pal, J.M.G.Y. Jiménez, F. Pérez-Rodríguez, Nanoscale Res. Lett. 7 (1) (2012) 1–12.

[9] Q.B. Li, J.M. Lin, J.H. Wu, Z. Lan, Y. Wang, Electrochim. Acta 56 (2011) 4980–4984.
[10] M. Saif, J. Photochem. Photobiol. A Chem. 205 (2009) 145–150.
[11] W.N. Wang, W. Widiyastuti, T. Ogi, I.W. Lenggoro, K. Okuyama, Chem. Mater. 19 (2007) 1723–1730.
[12] J.B. Yin, X.P. Zhao, Mater. Chem. Phys. 114 (2009) 561–568.
[13] A.K.A. Gafoor, J. Thomas, M.M. Musthafa, P.P. Pradyumnan, J. Electron. Mater. 40 (2011) 2152–2158.
[14] C.M. Gao, H.W. Song, L.Y. Hu, G.H. Pan, R.F. Qin, J. Lumin. 128 (2008) 559–564.
[15] V. Kiisk, V. Reedo, M. Karbowiak, M.G. Brik, I. Sildos, J. Phys. D Appl. Phys. 42 (2009) 125107 1–6.
[16] R. Liu, W.D. Yang, L.S. Qiang, J. Power Sources 199 (2012) 418–425.
[17] L.L. Lu, R.J. Li, T.Y. Peng, K. Fan, K. Dai, Renew. Energy 36 (2011) 3386–3393.
[18] J.H. Wu, G.X. Xie, J.M. Lin, Z. Lan, J. Power Sources 195 (2010) 6937–6940.
[19] H. Hafez, M. Saif, M.S.A. Abdel-Mottaleb, J. Power Sources 196 (2011) 5792–5796.
[20] T. Sekino, D.J. Park, J.Y. Kim, S.I. Tanaka, Mater. Integr. 25 (2012) 17–24.